TSDC and the Role of Space Charge in Polyacrylonitrile/Methylacrylate Copolymer Films

M. D. MIGAHED,* M. ISHRA, A. EL-KHODARY, and T. FAHMY

Polymer Laboratory, Department of Physics, Faculty of Science, Mansoura University, Mansoura, Egypt

SYNOPSIS

Space charge effects on direct current (DC) conductivity and the thermally stimulated depolarization current (TSDC) in the semicrystalline polyacrylonitrile–methylacrylate [P(AN–MA)] films have been investigated. The conduction was found to be controlled by space charge limited effect. On the other hand, the TSDC studies point to a superposition of dipole orientation and space charge effects. With the aid of the thermal sampling technique, the complex spectrum could be resolved into its elementary processes. Curve fitting has been carried out and peak parameters were determined. Information related to the motion of dipolar groups could be obtained. The compensation effects is observed to be valid and the value of the compensation temperature (T_c = 343 K) greatly differs from the glass transition temperature (T_g = 383 K). From the DC and TSDC studies considerations, the origin of the three conduction regions appearing in the ln σ vs. $1/T$ could be explored.

INTRODUCTION

In recent years, considerable interest has been paid to polymers. Special attention is devoted to obtaining intermediate properties with respect to homopolymers.[1–5] Conductivities of a variety of polymers have been measured, and it is found that the conduction at room temperature follows, in most cases, the normal Ohm's law. In other cases many dielectric materials are capable of carrying electric current by virtue of the injection of carriers at one or both the electrodes. Such conduction involves the existence of space charge in the body of the polymer and is thus distinct from ordinary Ohm's conduction. Many electrical properties of organic molecular solids are dependent on injection of carriers from electrodes[6,7] and the understanding of charge transport mechanism in these materials stem from the practical importance in fields such as electret production, electrostatic recording, and electrical insulation.

The electrical conductivity in direct current and the thermally stimulated depolarization current (TSDC) techniques have been used to study the electrical properties of different copolymers.[1,8,9]

The present study reports our experimental results of the effect of space charge on electrical conduction in the polyacrylonitrile–methylacrylate [P(AN-MA)] copolymer. Furthermore, we present TSDC studies to characterize the charge transport in this material. The thermal sampling (TS) technique was used, and it was found that the compensation rule is operative. Our results add further credence to the physical origin of compensation effect.

MATERIALS AND EXPERIMENTAL PROCEDURES

Acrylonitrile–methylacrylate copolymer (96% acrylonitrile and 4% methylacrylate, Polyscience, USA) is a semicrystalline material.[10] It consists of two segments: (i) acrylonitrile monomer, which contains a large number of highly polar CN groups, and (ii) methylacrylate monomer, which is a less polar and contains methyl group in the side branch. Films of thickness ranging from 10 to 150 μm were formed by both casting and pressing techniques. The material was dissolved in hot concentrated dimeth-

* To whom correspondence should be addressed.
Journal of Applied Polymer Science, Vol. 53, 1315–1322 (1994)
 CCC 0021-8995/94/101315-08

ylformamide (DMF). The solution was dried on a glass substrate under normal atmosphere at 323 K for one week. The cast film was annealed at 373 K for 24 h to reduce the content of DMF. On the other hand, press films were prepared by melting and pressing in a hot press at 420 K. Color changes in the film was observed above 465 K pressing temperature. Conducting surfaces of sample with 5 mm radius were prepared using conducting carbon paste (Neubauer Chemikalien, Germany), conducting silver paste (Conrady Nuernberg, Germany), aluminum, copper, and tungesten metal foils as electrodes. Details of experimental arrangements, measuring techniques, and curve fitting are to be found elsewhere.[1,8,11] Results were reproducible to within 10%.

RESULTS AND DISCUSSION

Conduction Current

Figure 1(a) shows the dependence of steady-state current–voltage (I–N) characteristics on electrode materials at room temperature. On the other hand, the isothermal log I–log V plot, at different temperatures, using carbon paste as electrodes, is displayed in Figure 1(b). The current values were measured for fields ranging from 8×10^4 to 3×10^6

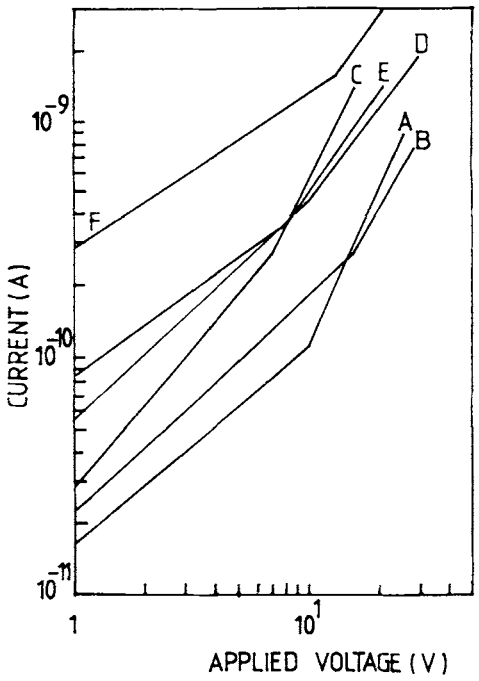

Figure 1(a) Current–voltage characteristics of P(AN–MA) films at 300 K for different electrode material configurations. Curves: (*A*) C–C; (*B*) Ag–Ag; (*C*) Ag(+)–C(−); (*D*) C(+)–Cu(−); (*E*) Cu(+)–C(−); (*F*) C(+)–Ag(−).

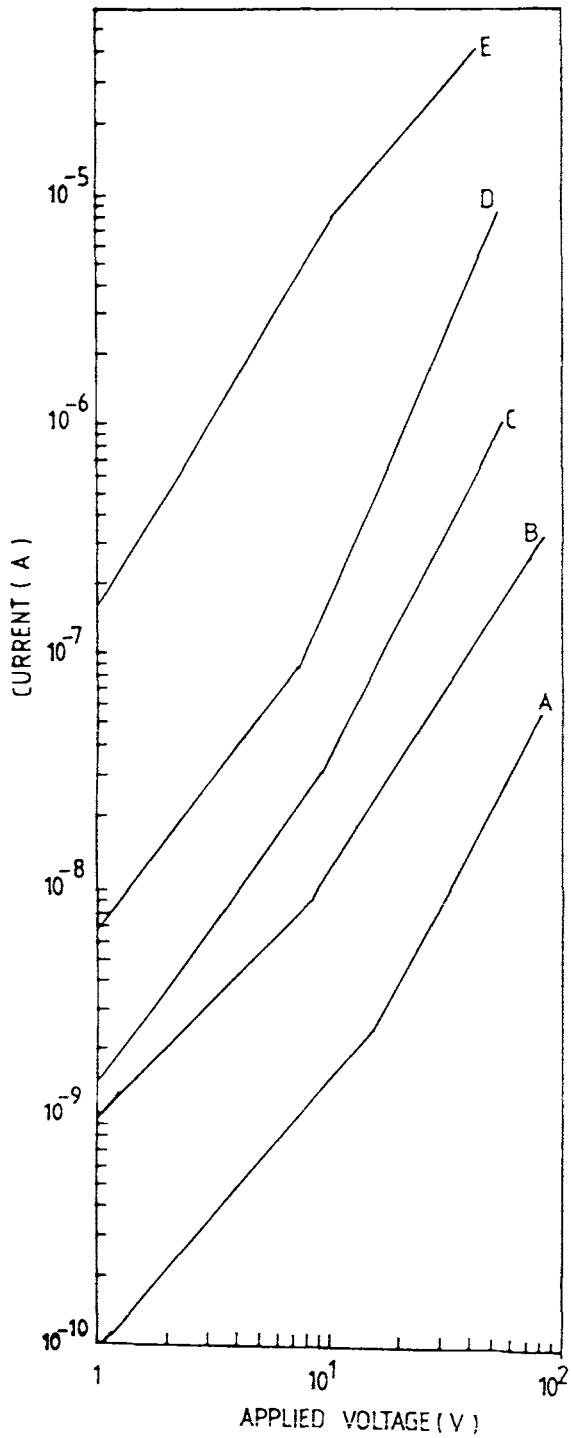

Figure 1(b) Temperature dependence of I–V characteristics for cast films of thickness 120 μm and with carbon paste as electrodes. Curves: (*A*) 333 K, (*B*) 343 K, (*C*) 353 K, (*D*) 383 K, (*E*) 393 K.

V/m. The slope value at low field and temperature is around 1, which indicates Ohmic behavior in this region. The change over in conduction from Ohmic to space charge limited is clear at high electric fields and temperature. Also as Figure 1(a) illustrates, the conduction current in the film with carbon electrodes differs from that with silver electrodes. On the other hand, the conduction current in the film with carbon anode is higher than that with silver anode, by at least one order of magnitude at low fields. Since the conduction, in the high field region, can be considered to be space charge injection limited as well as induced polarization, this must reflect the decrease in the slope of the current ($n > 1$) in this region.

The time dependence of the conduction current at constant temperature is shown in Figure 2. The solid curve represents the current–time relation after the application of the voltage. The dashed curve represents the same relation after the reversal of the polarity of the applied voltage.[12] As the time ellapses at constant applied field and temperature, the injected carriers sweep away to the counter electrode rather than forming homo space charge. Therefore, a transient current peak results as expected by the theory of the transient space charge limited current.[13] However, the intensity of the maximum current peak is not the same, which revealed that the current is partially consists of the release of deep trap charge carriers. The time corresponds to the maximum current peak (t_{max}) and is known as the relaxation time (t_r).[12] The drift mobility (μ) of charge carrier was derived from the relation;

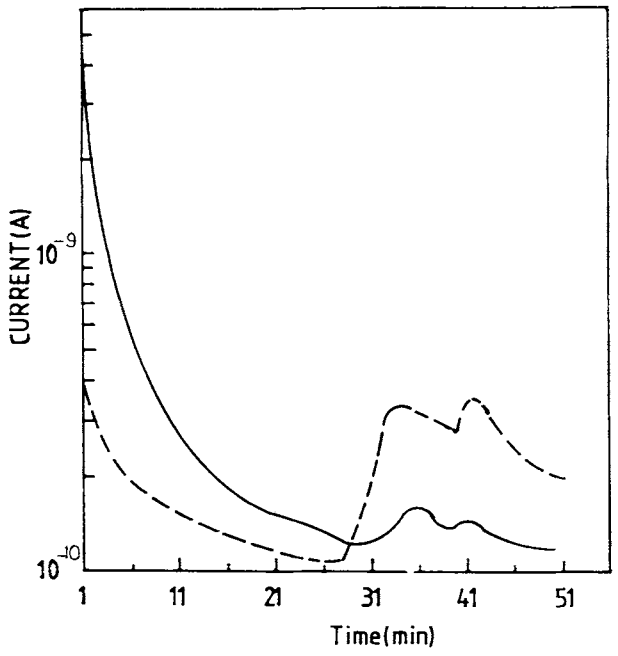

Figure 2 Transient current peaks in a cast film on applying the voltage (solid curve) and on reversing the polarity of the applied voltage (dashed curve). $E = 1 \times 10^6$ V/m, $T_p = 343$ K.

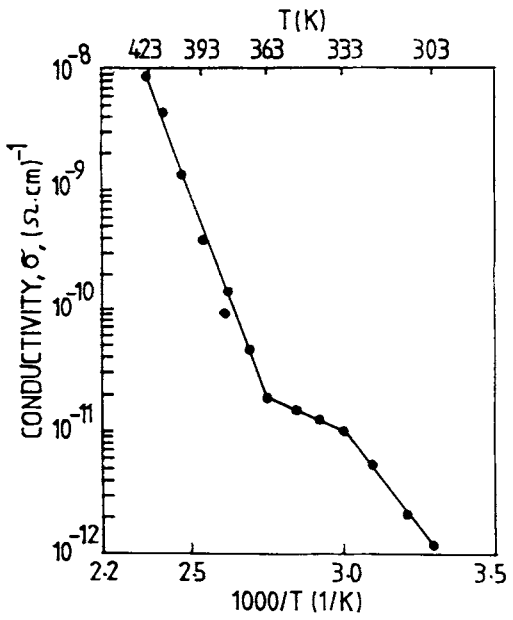

Figure 3 Conductivity, σ, vs. reciprocal of temperature, T, for a cast film, $E = 1 \times 10^5$ V/m, Film thickness = 150 μm, carbon electrode.

$$t_r \cong t_{max} = d^2/\mu V \quad (1)$$

where d is the thickness of the sample and V is the applied voltage. Mobility of $\cong 7 \times 10^{-15}$ m^2 V^{-1} s^{-1} at $T = 343$ K and field strength of 1×10^6 V/m was estimated, which is nearly independent of the applied voltage polarity. The value of μ depends on the experimental parameters such as applied voltage, film thickness, and temperature. The obtained μ at 343 K is in good agreement with the trap-modulated effective mobility that resulted from the surface potential decay curves.[5]

The variation of the conductivity, σ, with the reciprocal of temperature, T, at different field strengths is shown in Figure 3. The investigation of ln σ vs. $1/T$ at different electric fields revealed that the experimental results could be fitted by two or three intersection straight lines, the slope of which yield the apparent activation energy, E_a, according to the equation:

$$\sigma = \sigma_0 \exp(-E_a/kT) \quad (2)$$

where σ_0 is the preexponential factor and k is the Boltzmann constant. The intersection points depend, in general, on the film thickness and the applied voltage. Furthermore, the apparent activation energy of the low-temperature portion depends on the electrode materials. On the other hand, the apparent activation energy of the high-temperature portion ranges from 1.3 to 1.4 eV. This value is in good agreement with the results of Berlepsh et al.[5] The three slopes indicate that there are three different types of conducting mechanisms in P(AN-MA) in the temperature range 303–433 K.

In summary, direct current measurements clearly suggest that the conduction current in P(AN-MA) is dominated by charge injection. A non-Ohmic contact may act as a nearly Ohmic contact at low applied voltage by injection of carriers from electrode to the bulk of the material, but at an appropriate range of applied voltage and temperature it may act as a nearly blocking contact with the carrier supply limited by Schottky-type thermoionic emission. This nearly blocking behavior can be changed again to a nearly Ohmic behavior on increasing the applied voltage.

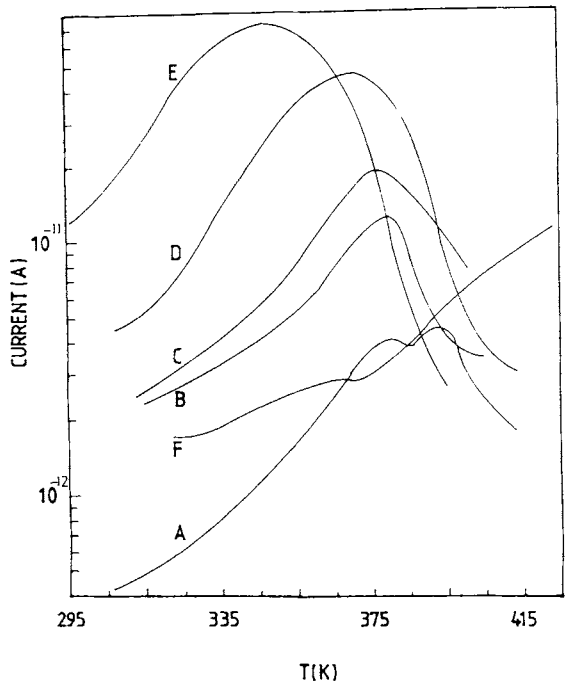

Figure 4 Family of short-circuited TSDC thermograms for cast and press-prepared films with various electrode materials, $E_p = 1 \times 10^6$ V/m, $T = 373$ K and $t_p = 1$ h. Press film: (A) carbon. Cast films: (B) tungsten, (C) aluminum, (D) carbon, (E) silver, and (F) second run of curve D.

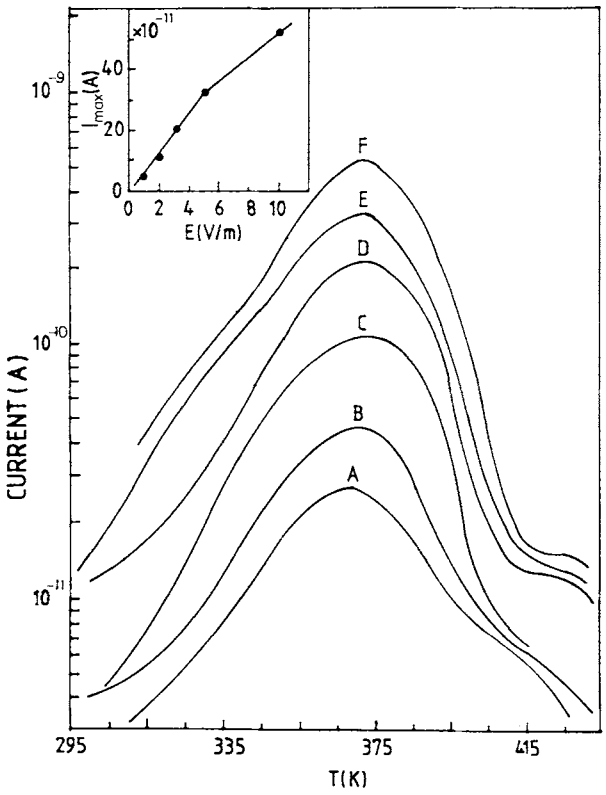

Figure 5 Family of short-circuited TSDC thermograms for cast film of thickness 15 μm polarized at 373 K for 1 h for various initial polarizing field. Curves A, B, C, D, and E correspond to E_p of 0.5, 1, 2, 3, 5, and 10×10^6 V/m, respectively. Heating rate $\beta = 3$ K/min. Carbon paste as electrodes.

Thermally Stimulated Depolarization Current

Figure 4 illustrates a set of curves obtained for polarized films at a poling field $E_p = 1 \times 10^6$ V/m, and a poling temperature $T_p = 373$ K for 1 h using different electrode materials. The heating rate (β) was 3 K/min. As it is clear, we can note the existence of only one peak in case of cast-prepared films, instead of two peaks in case of press-prepared film (see curve A). Furthermore, the peak position, T_m, is nearly the same in case of aluminum, carbon, and tungsten as electrodes. However, in case of silver paste as electrodes, T_m is shifted to the lower temperature side (curve E) and a prominent peak at about 348 K is obtained, which is comparable with the results of Berlepsch et al.[5] The first run, for the electret having carbon electrodes (curve D) was followed by a second one (curve F). Whereas the peak is just discernible as a weak shoulder, a residual current appears at $T \cong 373$ K reflects the retrapping of charge carriers.

Figure 5 represents a family of TSDC thermo-

grams obtained after poling for 1 h at T_p = 373 K for different initial applied fields. All spectra exhibit more or less the same shape. The height of the current maximum, I_m, is a nonlinear function of the polarized field E_p as shown in the inset of the figure. The peak position, T_m, and the average activation energy, E_a, of the discharge process, as determined by the first rise method,[14] remain nearly unaltered for all values of field strength. Investigation of TSDC spectra for P(AN–MA) films poled at t_p = 1 h with $E_p = 5 \times 10^6$ V/m and corresponding to different initial poling temperature, T_p, illustrated that the curves exhibit, nearly, the same character. However, there is no exact behavior for the amplitude of the current peak, I_m, with the poling temperature. Table I shows that the peak parameters depend on T_p. Furthermore, I_{max} depends on the polarizing time. It increases as t_p increases up to 1 h for films poled at $E_p = 5 \times 10^6$ V/m and T_p = 373 K.

The peaks observed in TSDC experiments are often too broad and obviously composed of several elementary peaks. The use of partial heating technique, which is believed to enable one to resolve overlapping peaks due to discrete relaxations or to study energetic distributions of relaxation processes, did not evince more than one current peak. Again T_m, E_a, and τ_0 of the resolved peak depend on the poling parameters as shown in Table II.

In summary, the global TSDC spectrum is often too broad to be attributed to a single relaxation frequency. The TSDC studies point to a superposition of dipole orientation and space charge effects. Since the apparent activation energy critically depends on T_p (see Table I), a distribution in both the relaxation time and the activation energy is to be expected.

The investigation of complete TSDC spectrum in Figure 5 shows the existence of various relations in the copolymer, but this spectrum is generally complex and only its resolution can provide information on the various processes. Such a resolution could be performed by the TS technique.[8] This technique is often of great potential and it has been used to decompose the whole TSDC spectrum in elementary contributions, which can be seen in Figure 6. As it is clear, 11 elementary peaks were obtained with a temperature window, T_w, = 5 K.

Nine of them can be considered as single Debye peaks. The last two peaks, which appear at the highest temperatures are mixed peaks. A curve fitting[11] has been carried out for all TS peaks, and Figure 7 illustrates a typical depolarization response to a TS program. Relaxation times obtained for the Debye peaks by this procedure are Arrhenius-like, and the corresponding peak parameters E_a and τ_0 are listed in Table III.

Table I Peak Parameters of the Global Spectra in P(AN–MA)

T_p (K)	T_{max} (K)	E_a (eV)
333	357	0.4920
353	361	0.5430
363	363	0.4860
373	371	0.4910
383	380	0.5690
393	379	0.7550
403	385	0.8210

Table II Characteristic Dependence of the Isolated Peak on the Poling Parameters, Carbon Paste as Electrodes, $E_p = 2 \times 10^6$ V/m

Exp. No.	T_p (K)	t_p (min)	T_m (K)	E_a (eV)	τ_0 (s)
1	353	60	102	1.12	3.0×10^{-13}
2	373	60	116	1.74	4.3×10^{-21}
3	373	10	112	1.62	9.8×10^{-20}
4	413	60	124	1.02	5.5×10^{-11}
5[a]	373	60	104	1.04	7.5×10^{-12}

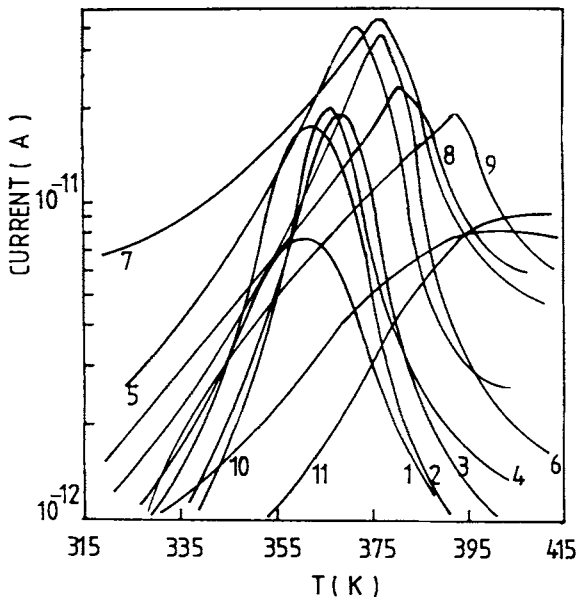

Figure 6 TSDC spectrum of P(AN–MA) cast film (*A*) of thickness 15 μm for 1 h with $E_p = 5 \times 10^6$ V/m, T_p = 393 K. An 11-TS curve corresponding to T_p of 333, 338, 343, 348, 353, 358, 363, 368, 373, and 378 K respectively. β = 3 K/min and carbon paste as electrodes.

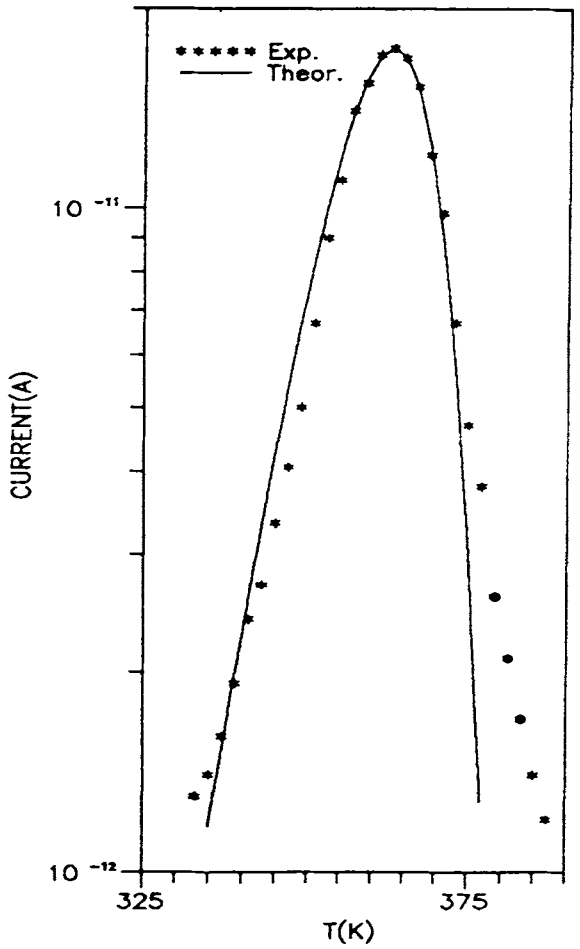

Figure 7 Typical fitted curve of a depolarization response to a TS program of P(AN-MA). T_p = 333 K, t_p = 15 min, T_c = 328 K, $E_p = 5 \times 10^6$ V/m, β = 3 K/min. (TS experiment no. 3 in Fig. 6).

Compensation Effect

Assuming a single relaxation time for each of the elementary peaks, the relaxation time, $\tau(T)$ can be obtained from the Arrhenius equation:

$$\tau(T) = \tau_0 \exp(E_a/kT) \qquad (3)$$

where τ_0 and E_a are known from the curve fitting.

If the compensation law, i.e., a linear relationship between ln τ_0 and E_a exists, hence the above expression becomes

$$\tau(T) = \tau_c \exp\{(E_a/k)[(1/T) - (1/T_c)]\} \qquad (4)$$

where τ_c and T_c are known as compensation time and compensation temperature, respectively.

The plot of ln τ vs. $1/T$ shows the dependence of activation energy on temperature. Figure 8 shows the least-squares fitting of the plots from the TS responses. It is clear that in the diagram showing τ against $1/T$ most Arrhenius plots pass through a common point located at $T = T_c$ and $\tau = \tau_c$, suggesting a compensation law in the case of the studied copolymer. T_c and τ_c have the values 343 K and 6.9 $\times 10^3$ s, respectively. The compensation temperature is widely far from the glass transition temperature ($T_g \cong 383$ K as determined by differential scanning calorimetry). As observed before (see Fig. 2), a transient peak was observed at the temperature T = 343 K. The agreement between T_c and this temperature encourages us to suggest that the compensation temperature is related to the dipole relaxation. The observed compensation temperature does not agree with the previous observations that such a compensation law generally accompanies the glass transition with a compensation temperature closely related to the glass transition temperature.[15]

Table III illustrates the calculated values of τ_0 from the equation.[16]

$$\tau_c = (kT_m^2/\beta E_a)\exp(-E_a/KT_m^2) \qquad (5)$$

where T_m is the temperature at which the TS peak is maximum and the other parameters have the same

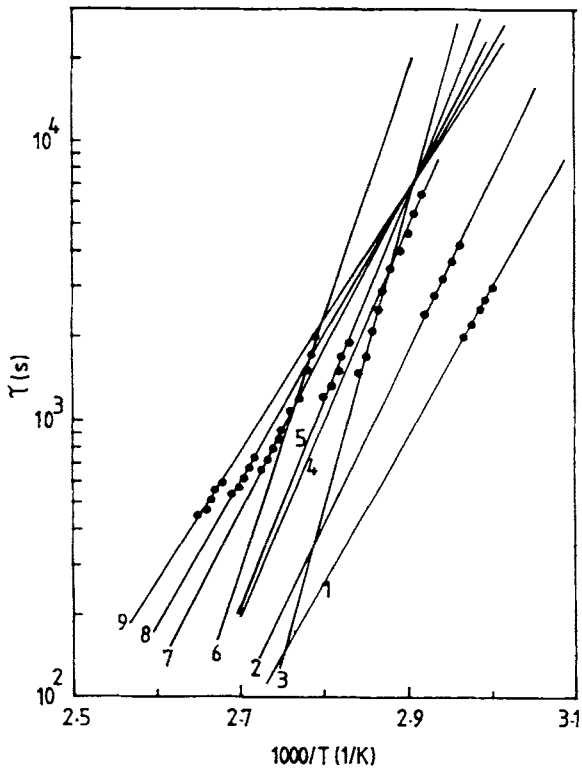

Figure 8 Variation of the relaxation times, τ, with the reciprocal of the temperature, T, for the elementary spectra 1–9 obtained from TS experiments.

meaning as given before. When ln τ_0 is plotted vs. E_a, one linear relationship is required to fit the elementary processes as shown in Figure 9.

The most interesting outcome to be drawn from Figure (9) is that all relaxation results for P(AN–MA) obey one single relaxation. It seems that all elementary processes can be ascribed to a dipolar polarization associated with micro-Brownian motion in the amorphous phase. The compensation temperature would be related to the transfer of heat in agreement with the idea developed by Peacock-Lopez et al.[17] who suggested that T_c is characteristic of the heat transfer between the thermal bath and the polymer chain. The interface regions are also of importance, since the trapped carriers are supposed to be located in the crystalline amorphous interface region. Hence, the high-temperature peaks (TS 10 and 11 in Table III) can be attributed to space charge relaxation process associated with the release of the deep trapped charge carriers.

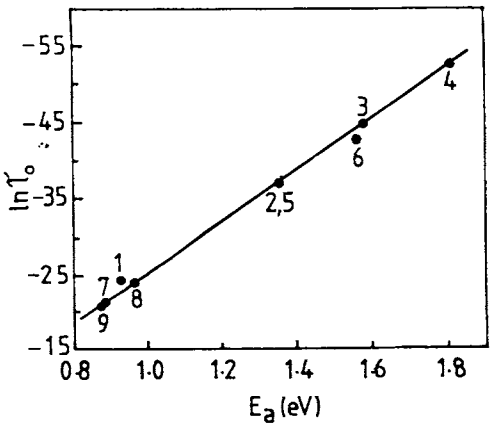

Figure 9 Variation of ln τ_0 vs. activation energy for the elementary process of complex spectrum of P(AN–MA). The numbers on the straight line indicate TS experiment numbers.

CONCLUSION

The conduction in P(AN–MA) is influenced by the injection intensity of the charge carriers in the P(AN–MA) copolymer. The importance of the crucial influence of injected carriers on electrical properties and relaxation processes has been evidenced. At higher voltages, the current is mainly carried by the injected charges. Carriers injected into the polymer, localized at deep defect levels, generate an inhomogeneous and nonstationary space charge exhibit as an electret in the polymer.[18] Thermal sampling technique allowed us to resolve the complex TSDC spectrum into its elementary processes and to differentiate between dipole and space charge relaxations. The observed compensation effect assert that P(AN–MA) presents compensation law with a compensation temperature far from its glass transition temperature. Its existence could be explained by the dipolar relaxation in the crystalline region. The investigations showed evidence for three conduction mechanisms and also three relaxations. The high-temperature one ($T > 363$ K) could be attributed to nonpolar processes associated with the movement of the detrapped charge carriers from the interfaces. The middle temperature region may be due to dipolar polarization, i.e., dipolar reorientation of the strongly polar character of the nitrile group (CN) with a dipole moment of about 3.5 Debye in the crystal defects. The low-temperature mechanism ($T < 333$ K) may be associated with local chain motion in the amorphous phase.

Table III Characteristic Parameters Obtained from TS Peaks Isolated in the Complex Spectrum of P(AN–MA)

TS No.	T_w (K)	T_m (K)	E_a (eV)	τ_0 (s)
1	338–333	361	0.93	2.5×10^{-11}
2	343–383	363	1.36	2.2×10^{-17}
3	348–343	369	1.58	3.9×10^{-20}
4	353–348	367	1.81	1.8×10^{-23}
5	385–353	373	1.36	7.4×10^{-17}
6	363–358	377	1.56	2.2×10^{-19}
7	368–363	379	0.89	4.1×10^{-10}
8	373–368	381	0.97	3.8×10^{-11}
9	378–373	383	0.88	7.6×10^{-10}
10	383–378	—	—	—
11	388–383	—	—	—

REFERENCES

1. M. D. Migahed, A. Tawansi, and N. A. Bakr, *Eur. J. Polym.*, **18,** 975 (1982).
2. T. Furukawa, J. X. Wen, K. Suzuki, Y. Takashina, and M. Date, *J. Appl. Phys.*, **56,** 928 (1984).
3. D. Ronarch, P. Audren, and J. L. Moura, *J. Appl. Phys.*, **58,** 466 (1985).
4. Y. Suzuoki, H. Muto, T. Mizutani, and M. Ieda, *J. Phys. D: Appl. Phys.*, **20,** 1053 (1987).
5. H. von Berlepsch, M. Pinnow, and W. Stark, *J. Phys. D: Appl. Phys.*, **22,** 1143 (1989).
6. K. C. Kao, W. Hwang, *Electrical Transport in Solids,* Oxford; Pergamon, Chap. 2; (1981).
7. M. Pope and C. E. Swenborg, *Electronic Processes in*

Organic Crystals, Oxford, Clarendon, Chap. II, Sec. E, 1981.
8. M. D. Migahed, A. Shaban, A. El-Khodary, M. Hammam, and H. R. Hafiz, *J. Polym. Mat.,* **7,** 131 (1990).
9. M. D. Migahed, A. El-Khodary, M. Hammam, A. Shaban, and H. R. Hafiz, *J. Mat. Sci.,* **25,** 923 (1990).
10. M. D. Migahed, F. M. Reicha, M. Ishra, and M. El-Nimer, *J. Mat. Sci.: Mat. Electro.* **2,** 146 (1991).
11. M. D. Migahed, H. R. Hafiz, A. Shaban, and M. Ishra, *J. Polym. Mat.,* **8,** 329 (1991).
12. A. Many and G. Rakavy, *Phys. Rev.,* **126,** 1980 (1962).
13. S. Isoda, H. Miyaji, and K. Asi, *Jpn. J. Appl. Phys.,* **12,** 1799 (1973).
14. G. F. J. Garlick and G. F. Gibson, *Proc. Phys. Soc.,* **60,** 547 (1948).
15. C. Lacabanne, D. Chatain, J. C. Monpagens, A. Hiltner, and E. Baer, *Solid State Commun.,* **27,** 1055 (1978).
16. M. M. Perlman, *J. Appl. Phys.,* **24,** 2645 (1971).
17. E. Peacock-Lopez and H. Suhl, *Phys. Rev.,* **B26,** 3774 (1982).
18. G. M. Sessler, *ed.*, *Electrets,* Berlin, Springer, 1980.

Received September 15, 1993
Accepted January 22, 1994